Opportunity of DC technology for powering pipe-in-pipe heating system

Duvan Mendoza Lopez, Zakaria Lettifi, Léo Sudriès, Christian Geertsen, Emmanuel Perez, Laurent Berquez, Gilbert Teyssedre

▶ **To cite this version:**

Duvan Mendoza Lopez, Zakaria Lettifi, Léo Sudriès, Christian Geertsen, Emmanuel Perez, et al.. Opportunity of DC technology for powering pipe-in-pipe heating system. 11th International Conference on Insulated Power Cables, Jun 2023, Lyon, France. hal-04310683

HAL Id: hal-04310683
https://hal.science/hal-04310683

Submitted on 27 Nov 2023

HAL is a multi-disciplinary open access archive for the deposit and dissemination of scientific research documents, whether they are published or not. The documents may come from teaching and research institutions in France or abroad, or from public or private research centers.

L'archive ouverte pluridisciplinaire **HAL**, est destinée au dépôt et à la diffusion de documents scientifiques de niveau recherche, publiés ou non, émanant des établissements d'enseignement et de recherche français ou étrangers, des laboratoires publics ou privés.

Opportunity of DC technology for powering pipe-in-pipe heating system

Duvan **MENDOZA LOPEZ**, Zakaria **LETTIFI**, Léo **SUDRIÈS**, Christian **GEERTSEN** and Emmanuel **PEREZ**, ITP Interpipe, Louvenciennes (France), duvan.mendoza@laplace.univ-tlse.fr, zakaria.lettifi@outlook.fr, sudries@insa-toulouse.fr, christian.geertsen@itp-interpipe.com, emmanuel.perez@itp-interpipe.com

Laurent **BERQUEZ** and Gilbert **TEYSSEDRE**, University of Toulouse and CNRS, Toulouse (France). laurent.berquez@laplace.univ-tlse.fr, gilbert.teyssedre@laplace.univ-tlse.fr

ABSTRACT

The risks associated to a change in technology for heating system in pipe-in-pipe flowline technologies is evaluated. We show that the field distribution under DC stress is markedly different from that in case of AC stress owing to the high electrical conductivity of the splice joint insulation relatively to cable insulation. Model structures were used to investigate multilayer samples. Safe conditions regarding space charge accumulation were addressed. Finally, the field distribution in real joints was estimated considering the actual geometry. All in all, the results show that the cables can safely be operated under DC with at least same voltage as under AC stress.

KEYWORDS

Special cables, insulating polymers, DC stress, offshore environment

INTRODUCTION

In some applications like offshore oil and gas transportation for example, fluids need to be transported over very long distances and may require electrically heated flow lines to facilitate the transfer. Pipe-in-pipe flowline technologies have been developed for this purpose, consisting in an inner pipe enclosed with a cable heating system and a very good thermal insulation inside a second outer pipe [1]. This technology is known as Electrical Heat Traced Flowlines (EHTF) and is shown in Figure 1 [2]. The heating system is provided by cables strung out along the pipe with joints to be formed between pipelines sections of typically 1.5 km long. The thermal insulation is ensured by combining a physical aerogel with de-pressurized environment in the inter-pipe spaces.

Historically, the cables are supplied with AC voltage for simplicity of supply, but a novel approach using DC voltage is under consideration as it would reduce or even eliminate some of the failure modes related to AC, notably partial discharges (PD)-driven degradation processes. PD harmfulness is enhanced by the low-pressure environment, due both to the decrease of the inception voltage when decreasing the pressure and to the increase in the energy of the discharge [3]. Additionally, moving to DC powering would also eliminate the capacitive losses over long distances, thus improving reach from a single point of supply.

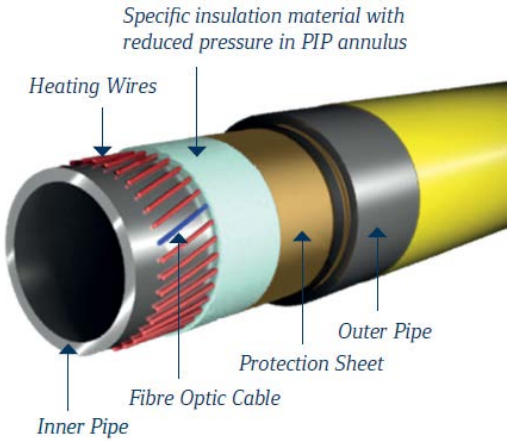

Fig. 1: Typical cross section of an EHTF system [2]

For the present application, the system is normally not operated at temperatures higher than 50°C. However, it can be exposed to higher temperatures (130°C) under flowing conditions. Therefore, materials must support such stresses.

With moving to DC, it is expected that the performances and reliability of the heating system could be improved. It is however important to study whether other degradation of failure scenarios occur due to the DC stress. Notably, the electric field distribution under DC stress is usually markedly different from that in case of AC stress owing to the resistive field grading within the insulations. Ensuring high reliability is all the more important as in the specific case of offshore pipe-in-pipes, the heating system has to function for decades with no possibility for repair. The design for the lifetime of such a heating system taking into account probability of failure of each splice is treated in another paper in this conference [4].

The objective of the research reported in this work is to estimate the potential new risks in powering existing cable technologies in DC, and to explore limit conditions. The cables used in the system are insulated with a thermostable polymer. Joints are manufactured by heat-shrinking tubes of semiconductor and insulations on splices. As in power cables, the joints a priori constitute weak points to the cable heating system. Therefore, focus is put on the behavior of the joints under DC stress and on possible failure due to the assembly.

HEATING CABLE STRUCTURE

Lay-out

Figure 2 shows a drawing of the cable structure and of a joint also called *splice*. The cable itself is made of copper conductor and Fluorinated Ethylene-Propylene copolymer (FEP) of 0.65mm thickness as bulk insulation. Semiconducting layers (semicon) are present on the conductor and on the outer part of the cable. In this way, the potential difference between the outer part of the cable and the inner pipe on which it is wound is low and the PD occurrence is minimized.

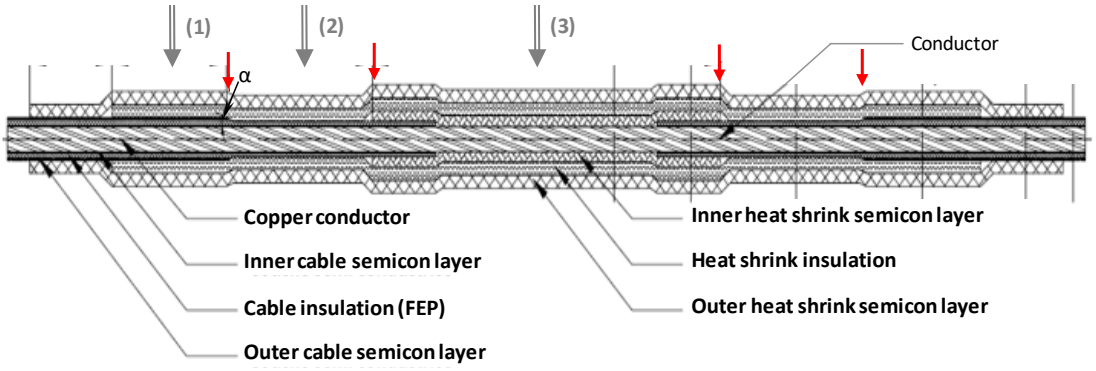

Fig. 2: Schematic drawing of a splice of total length 13.5mm. The conductor crimp connector is not represented. Red arrows indicate potential fragile points.

Typical voltages are 1.1 kV_{AC} (well above partial discharge inception voltage at the annulus pressure condition) with an aim to achieve 3-6 kV in DC.

To join two sections of cables, the outer semiconductor is stripped and removed over a few centimeters. The two conductors are assembled using a crimp connector. Then, the 3 are functionally reinstated, starting with a semicon, an insulating layer and ending with a semicon, all three layers being heat-shrinkable. The heat-shrinkable insulation covers the semicon on the crimp connector and the outer semicon of the cable. The outer semicon layer ensures electrical continuity at the surface.

From the drawing of Figure 2, several potential weak points can be identified. Leakage may appear at the surface of the stripped cable, if adhesion between the heat-shrink semicon and the FEP layer is not satisfactory. Second, there are regions of field reinforcement (triple points) at the junction of cable insulation, crimp semicon and heat-shrink insulation, with even potentially the presence of air. These regions are indicated as red arrows in Figure 2. Finally, the electrical properties of the materials, notably the heat-shrinkable ones, are not known. From these properties depend the field distribution.

In order to provide more knowledge about these effects, the field distribution in a simplified splice has been computed, focusing on hot points that may appear in the joint. This has led to the need to get data on the conductivity of the different layers. Therefore, leakage currents have been measured on a real splice and on single layers of heat-shrinkable materials. Finally, space charge measurements have been tentatively realized on single and multilayers.

Materials analysis

On the material side, while the cable is relatively well identified, little was known about the behavior of heat-shrinkable materials. For this reason, detailed structure and thermal properties were investigated.

First, cross-sections were taken at different places along a splice as indicated in Figure 2 and analyzed by optical microscopy. Figure 3 shows an example of cross-section, revealing besides the semicon, the existence of a double layer within the insulation. This double layer appears as an adhesion, hot-melt layer usually achieved with EVA (ethylene vinyl acetate) or polyamide resin [5]. The distribution of the thicknesses of the various layers vary according to the position along the splice due to the profile of the underlayers. Hence, the minimum thickness of

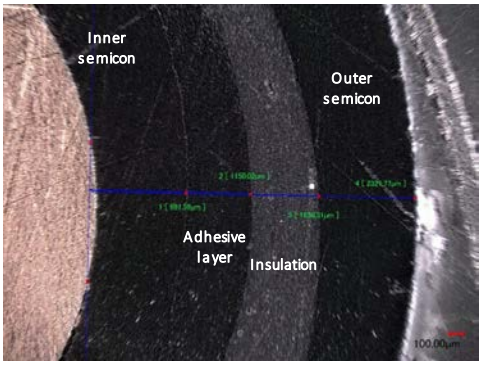

Fig. 3: Example of cross-section revealing from left to right: heat-shrink semicon, adhesive layer, insulation, outer semicon. Total thickness: ≈2mm

insulation layer is found on the crimp connector. The total thickness of heat-shrink materials is around 1.8mm.

Position	Full cable (1)	Stripped cable (2)	Middle (3)
Outer sc	0.95±0.05	0.90±0.05	0.60±0.15
Insulation	0.70±0.05	0.65±0.05	0.50±0.10
Adhesive	0.35±0.05	0.30±0.05	0.25±0.05
Inner sc	/	/	0.45±0.10

Table 1: Thicknesses of heat shrink material layers (in mm) measured at different positions in a splice as indicated in Fig. 2.

The thermal properties of the materials were analyzed using differential scanning calorimetry. The melting and crystallization temperatures for the insulation (without adhesive) was found at 81.7°C, the crystallization temperature at 65.2°C, see Figure 4. These values and the low crystallinity degree (about 10% based on the melting enthalpy of Low Density Polyethylene) are compatible with Very-Low-Density Polyethylene (VLDPE) a material commonly used for heat-shrink applications [6, 7]. For the semicon, the melting and crystallization temperatures were respectively 99°C and 84°C.

Of importance here is the realization that the heat shrink materials used for the manufacturing of splices have a low melting point, for the purpose of avoiding too much heating of the substrate on which they are applied. As the ambient temperature may be higher than the melting point, their long term behavior should be investigated.

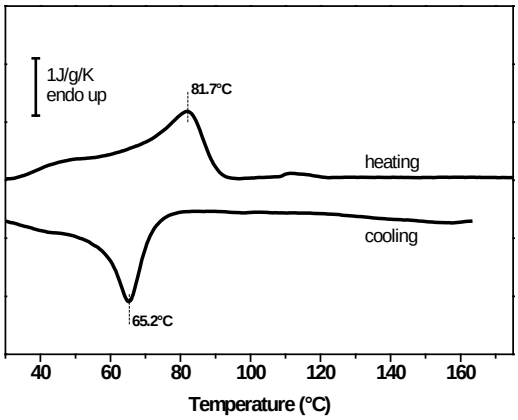

Fig. 4: DSC thermograms obtained on adhesive-free heat-shrink insulation during heating/cooling up to 180°C at 10°C/min.

ELECTRICAL CHARACTERISATION TEST RESULTS

DC field distribution in the splice

The preparation of the cable ends follows a particular stripping procedure in which two cuts are made to expose the conductor and the insulation. In Figure 5.a, two areas of interest and their characteristics are underlined. On the right side, we end up with an area on which is placed a heat shrink semicon layer and a heat shrink insulation layer leaving an air space at the interface of the 3 materials. On the left side, a cut with an inclination of 20° passes through the outer semicon layer of the cable and part of the insulating material. This configuration will allow the integration of the heat shrink insulating and semicon layers to establish the junction.

The electric field was computed in DC conditions, supposing a ratio between the electrical resistivity of the FEP cable insulation and that of the heat shrink insulation of about 10. The resistivity in the air was supposed to be less than in the insulations. The maximum geometric field in the FEP cable insulation away from the joint was 2 kV/mm. Fig 5.b shows the results for the field distribution in steady state for the two critical regions. In the specific conditions considered here, field intensification was greater at the cone cut. A maximum field of 13.5kV/mm was obtained in the cable insulation. The most suitable conditions for relaxing the field where determined with varying the angle of the cone. Actually using materials with different ratio of conductivity may change the result, the reason why the materials conductivity was investigated.

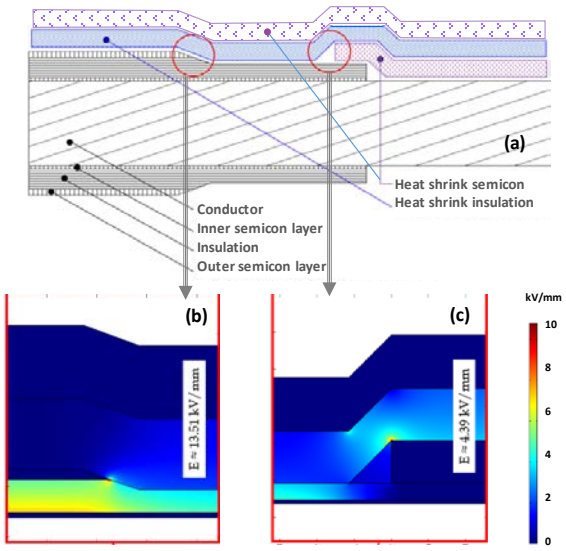

Fig. 5: a) Zoom of critical regions of the joints and field mapping obtained under steady state in these regions: b) on the cone cut and c) with an air gap.

Current measurements

Leakage current measurements were recorded on splices as well as sections of the cable provided with inner and outer semicons. For cables, the arrangement described in [8] has been used: the outer semicon of the cable was removed out of an active region of about 30cm length. Two ribbons serving as guard electrodes were place at 2cm from the end of the semicons. The high voltage, up to 20kV, was applied to the conductor and the current was measured from the outer semicon using a Keithley 617 ammeter. Table 1 reports obtained estimations of the conductivity with using charging times of 1h. FEP has an extremely high resistivity. When measurable, the conductivity does not change with the field up to an averaged field of 25kV/mm. Then, non-linearity can be detected at about 25kV/mm and 30kV/mm for temperatures of 90 and 70°C, respectively.

Temperature (°C)	Conductivity (S/m) E <25kV/mm	Conductivity (S/m) E = 37 kV/mm
90	3.5×10^{-17}	7.2×10^{-17}
70	1.8×10^{-17}	3.0×10^{-17}
50	1.0×10^{-17}	1.0×10^{-17}

Table 2. Conductivity of FEP insulation

The same kind of experiments were repeated on full joints installed on two sections of cables. Figure 6 shows the currents recorded for 1h time under different voltages. Comparatively, a much greater leakage current was recorded on the joint compared to the cable. The maximum current obtained for a voltage of 20kV and a temperature

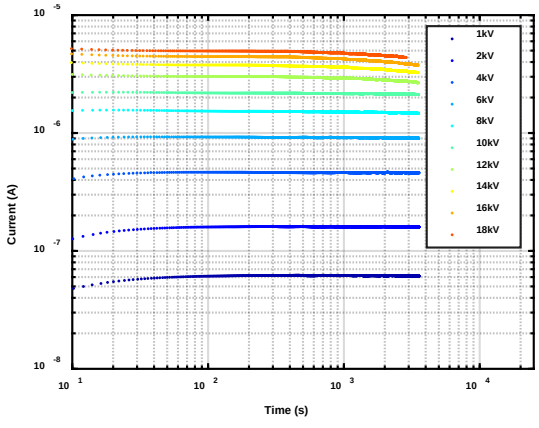

Fig. 6: Leakage current measured in a joint at different voltages at 50°C.

of 50°C for the 30cm-long FEP-insulated cable was 5pA, i.e. 5 orders of magnitude less than shown in Figure 6. Our first impression was that failure occurred in the joint, as for example leakage current at the interface between different layers. For that reason, a series of measurements was realized on model objects consisting in a heat-shrink insulation formed on a cable provided with a semiconducting layer that was used as high voltage electrode.

Figure 7.a shows examples of current transients obtained at 50°C on such arrangement. After a few minutes, a quasi-steady state current is reached, illustrating the relatively leaky character of the material. Under DC stress, the radial field distribution is of the form:

$$E(r) = \frac{V}{r.ln\left(\frac{r_e}{r_i}\right)} \quad [1]$$

Where r_i = 3.57mm and r_e = 4.35mm are the inner and outer diameter of the insulation. V is the applied voltage. The conductivity was estimated from:

$$\sigma = \frac{I}{\ell.2\pi.r_i.E(r_i)} \quad [2]$$

Where ℓ is electrode length and I the measured current.

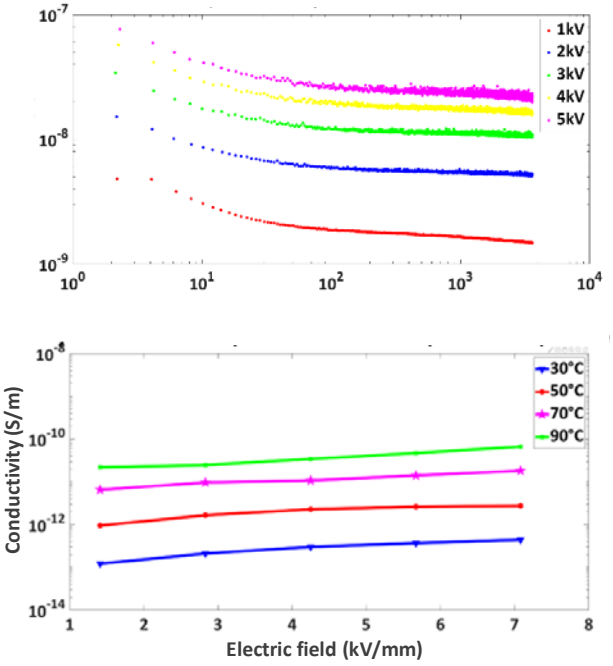

Fig. 7: (a) Transient charging current for heat-shrink insulation at 50°C for different voltages; (b) Conductivity values vs. field and temperature estimated from the current after 1h charging time.

Conductivity obtained for the heat-shrink insulation are represented in Figure 7.b as a function of the field and temperature. They are fully consistent with those estimated based on currents on the full joint, confirming that the leakage in the FEP is negligible and that the relatively high leakage current in the joint is not due to surface leakage. The conductivity weakly increases with the field at all temperatures. The relation between conductivity, field and temperature can be approximated by:

$$\sigma(E,T) = \sigma_0.\left(\frac{E}{E_0}\right)^n \exp\left(\frac{-\Delta}{k_b.T}\right) \quad [3]$$

With σ_0 =4S/m for E_o=1.4kV/mm, n=0.7, k_b=1.62 ×10^{-5}eV/K is the Boltzmann constant and Δ=0.81eV is the activation energy for conduction.

Space charge measurements

Obtaining space charge and electric field distributions in accessories such as those investigated here would be interesting for different reasons. First, it could allow identifying non-linear conduction regime if the field distribution deviates from a capacitive one, and resolving the field distribution in multilayer insulating structures. It may allow revealing space charge accumulation and would be useful to check how far charges generated by the material e.g. by PD occurrence are persistent. Recently, the group of N. Hozumi reported on charge distribution measurements at different positions within high voltage cable joints using an array of sensors [9] with the Pulsed Electro-Acoustic (PEA) method.

Some preliminary measurements have been achieved with the current object using a PEA test cell adapted to cables with relatively thin insulations [10]. The difficulties here are the fact that the cables have a small diameter, the conductor in the joint is not smooth due to the crimp connector, materials with very strong contrast in electrical conductivity are associated, and their acoustic properties are not the same.

Figure 8 summarizes the specificities that were encountered when working with such objects:

-The outer semicon is relatively thick compared to the insulation thickness (see Table 1): significant absorption of acoustic waves may occur.

-A new phenomenon was revealed which is the generation of a strong acoustic signal at the interface between the semicon and the ground plate. This was not observed in a so clear way in semicon used in model power cables. The response seems independent of the DC voltage, and results purely from the pulse voltage. The reason seems to be the capacitive response of the semicon at high frequency. This contribution, which is called here electrostrictive contribution, can be removed by subtracting the response obtained with the voltage pulse only without any DC pre-stressing.

-The association of several dielectrics, including the adhesive layer brings complexity. The adhesive layer fills the gap between the heat-shrink material and the underlayers and therefore has not a homogeneous thickness. In the same way, the thickness of heat shrink material may vary with heating conditions and with the diameter of the underlayer.

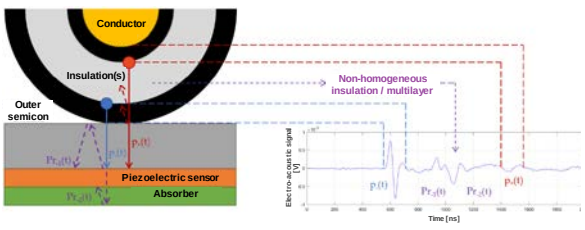

Fig. 8: Schematic of the electroacoustic response from a complex object as joint.

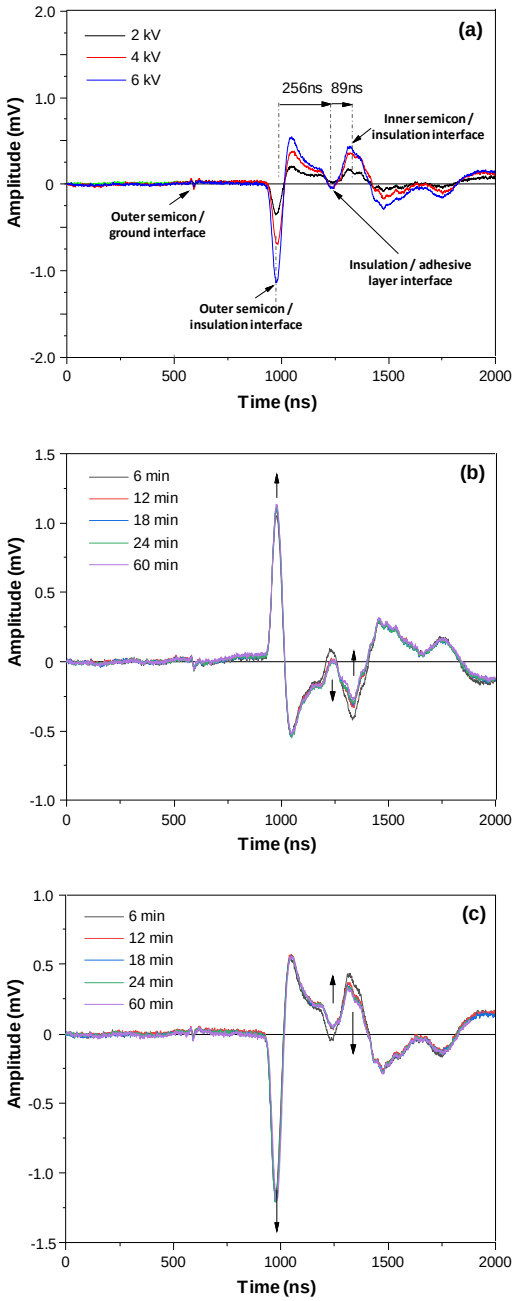

Fig 9: Rough electroacoustic signals obtained in the central part of a joint for different DC voltages: (a): short time (6min) after voltage application of 2, 4 and 6kV; During 1h under (b): -6kV and (c): +6kV.

Figure 9 shows the rough electroacoustic signal recorded on the central part of a joint for different applied voltages. The electrostrictive contribution has been removed and only a small residue, independent from the applied DC voltage can be noticed. The dip at about 1250ns has been considered as the interface between the heat shrink insulation and the adhesive. The propagation time of 256ns appears consistent with a heat-shrink insulation layer of about 500µm given the typical sound velocity of 2000m/s for polyethylene material. When changing the voltage, Figure 9.a, the signal has qualitatively the same shape.

When analyzing the time dependence of the signal (with 60min charging time, see Figures 9.b and 9.c), a mild evolution is detected: the peak at the outer semicon /insulation interface is slightly increasing and those in the middle and at the inner semicon interface tend to decrease. The response is very symmetric when changing the polarity of the applied voltage. These observations appear characteristic of a Maxwell-Wagner polarization phenomenon: it would result from a lower electrical conductivity for the heat-shrink layer compared to that of the adhesive layer, which is a very reasonable possibility.

The measurements could not be achieved on the part of the joint with cable insulation. For the cable alone, no charge could be detected for voltages up to 20kV.

To wrap-up about space charge measurements, no significant charge accumulation in the bulk of insulating layers was observed for applied voltages up to 6kV, which is well above the targeted service voltage. The clearest feature was an interfacial charge accumulation when associating materials having different electrical conductivities. The deconvolution, of the signal could not be further resolved due to the cylindrical geometry and the superposition of different layers whose acoustic properties and dimensions were not accurately known. The signal measured on the ground electrode can anyway provide a guess of field variation at this electrode, which reflects internal field redistribution due to space charge accumulation.

CONCLUSIONS

Some questions related to the change in technology from AC to DC for heating system in pipe-in-pipe flowline technologies were addressed. DC stress would reduce the risk of PD issues and would allow powering over longer distances. The multilayer nature of the insulation of the splices constituting joints between cables brings uncertainty for local field estimation. We showed that the heat shrink insulation used in joints has a much larger electrical conductivity than the insulation of the cable. Though leakage current seems relatively high, the splices seem to work safely under targeted service voltage. Short term breakdown tests reveal comfortable performances of the assembly.

To complete the study, and in view of the relatively low melting point of the joint materials, investigating the endurance of materials and joints at high temperature is forecasted. Also, the study should be completed by considering the depressurized environment. The used semicons have a capacitive response to transient voltage pulses and are presumably less conductive than typical semiconductors used in power cables. Their electrical properties deserve to be investigated in greater details.

REFERENCES

[1] C. Geertsen and M. Offredi, 2000, “Highly thermally insulated and traced pipelines for deepwater”, 12th Deep Offshore Technology Conference, 2000.

[2] A. Reveilloux, 2016, "From concept to commercialization: Market-ready electrically heat traced flowline", Deep7 Technology Magazine, vol. 7, pp. 8-9, may 2016.

[3] C. Emersic, R. Lowndes, I. Cotton, and S. Rowland, 2017, "The effects of pressure and temperature on partial discharge degradation of silicone conformal coatings", IEEE Trans. Dielectr. Electr. Insul., vol. 24, pp. 2986-2994.

[4] E. Perez and C. Geertsen, 2023, "Lifetime simulation and system reliability for Electrically Heat-Traced Flowlines (EHTF)", Proc. 10th Int. Conf. on Insulated Power Cables (JiCable), Lyon, France, June 2023.

[5] Y. J. Park and H. J. Kim, 2003, "Hot-melt adhesive properties of EVA/aromatic hydrocarbon resin blend", Internat. J. Adhesion Adhesives, vol. 23, pp. 383-392.

[6] B.L. Wilhoit, 1997, "Biaxially oriented heat shrinkable film", European Patent EP0562493B1.

[7] S. Yamasaki, T. Fujita, S. Nishikawa, Y. Emoto, R. Fujita, and S. Azuma, 2018, "Dual wall heat-shrinkable tubing with hot-melt inner layer", SEI Technical Review, N° 86, Apr. 2018, pp. 85-90.

[8] N. Adi, T. T. N. Vu, G. Teyssèdre, F. Baudoin, and N. Sinisuka, 2017, "DC model cable under polarity inversion and thermal gradient: Build-up of design-related space charge", Technologies, vol. 5, no 46.

[9] A. Tzimas et al., 2022, "Feasibility of space charge measurements on HVDC cable joints: Study Group—IEEE DEIS Technical Committee HVDC Cable and Systems", IEEE Electrical Insulation Magazine, vol. 38_5, pp. 18-27.

[10] A. Benyoucef, L. Berquez, G. Teyssedre and E. Aubert, 2020, "Space charge measurement by PEA on an aeronautical cable", Proc. IEEE Internat. Conf. on Dielectrics (ICD), pp. 351-354.